

## **Alternative divertor configurations – Physics basis and plans for ASDEX Upgrade**

T. Lunt<sup>1</sup>, O. Pan<sup>1</sup>, A. Herrmann<sup>1</sup>, D. Brida<sup>1</sup>, D. Coster<sup>1</sup>, P. David<sup>1</sup>, M. Faitsch<sup>1</sup>,  
Y. Feng<sup>1</sup>, M. Griener<sup>1</sup>, J. Hobirk<sup>1</sup>, D. Silvagni<sup>1</sup>, M. Wischmeier<sup>1</sup>  
and the ASDEX Upgrade, TCV and the EUROfusion MST1 Teams\*

<sup>1</sup>*Max Planck Institute for Plasma Physics, Garching/Greifswald, Germany*

### **Physics basis**

Power exhaust is expected to become a problem in a future fusion reactor based on the Tokamak design in single-null (SN) configuration [3]. As a potential solution, alternative divertor configurations are currently discussed and investigated by many laboratories in the world [4]. The potential benefits of these configurations rely on several physical effects: 1) The activation of additional strike points (SPs) in a ‘snowflake’ (SF) configuration [5] with the secondary X-point in the private flux region (SF+). This effect was partially observed in TCV, where a secondary SP received 10% of a primary one, i.e. about 10 times more than expected from pure diffusion ( $\sim 1\%$ ) [6]. A candidate that may cause this enhanced transport is the ‘churning mode’ postulated for the null-region of a SF [7]. Since it is unlikely that a 10% reduction of the peak load justifies the extra-costs of constructing a SF divertor, an interesting question is, whether the effect scales with machine size and/or  $\beta_{pol}$ . 2) a splitting of the power flux by introducing a secondary X-point in the SOL on the low-field side of the primary one (LFS SF-) and the corresponding additional diffusive transport occurring at the secondary separatrix [8]. This effect was observed experimentally in TCV by Langmuir probes [9, 10]. 3) an enhanced emission of SOL radiation of the LFS SF- compared to that of the SN [8], which in turn may allow 4) an easier access to detachment. A transition to detachment of the LFS SF- configuration at a lower density, seeding rate or a higher heating power compared to the SN was indeed observed in SOLPS simulations that recently became possible after fulfilling the technical requirement of the code that the physical grid needs to be mapped onto a block shaped computational grid [11]. Experimentally, the enhanced radiation in the region around the secondary X-point was observed in TCV [12] as well as an effect on the detachment, although rather on the degree of detachment than on the threshold for both the LFS SF- [12] and the X-divertor [13] configurations. 5) Finally the wetted area might be enhanced by increasing the poloidal flux expansion,

\*See the author lists of [1, 2]

although engineering constraints e.g. due to target tile positioning tolerances and/or error fields may set a limit [14].

### Plans for ASDEX Upgrade

In order to study a series of alternative configurations experimentally in a machine with a high heating power (30 MW) compared to its size ( $R=1.65$  m) and compare them to the conventional SN configuration, the installation of a couple of in-vessel coils in the close proximity of the upper outer strike-point (SP) of ASDEX Upgrade (AUG) is currently in preparation. In 2017 [14] we reported on the initial proposal and idea of the project at that time. In the meantime many engineering constraints – in particular those given by the mechanical and electrical safety against disruptions – were identified and the upgrade plans are much more advanced [15]. 2D and 3D plasma transport simulations were carried out recently [16] to study the actual coil design including the current feeds. Based on these studies the

exact (3D) conductor guiding was optimized. Its installation requires winding inside the machine including complex and accurate 3D bending.

In addition to these design studies, a series of USN discharges were now executed in AUG with the goal of testing and optimizing the reference equilibrium as well as to characterize well the plasma parameters and in particular those in the SOL when approaching detachment. Fig. 1 shows several time traces of the AUG USN H-mode discharge 36283 at  $I_p = 800$  kA plasma

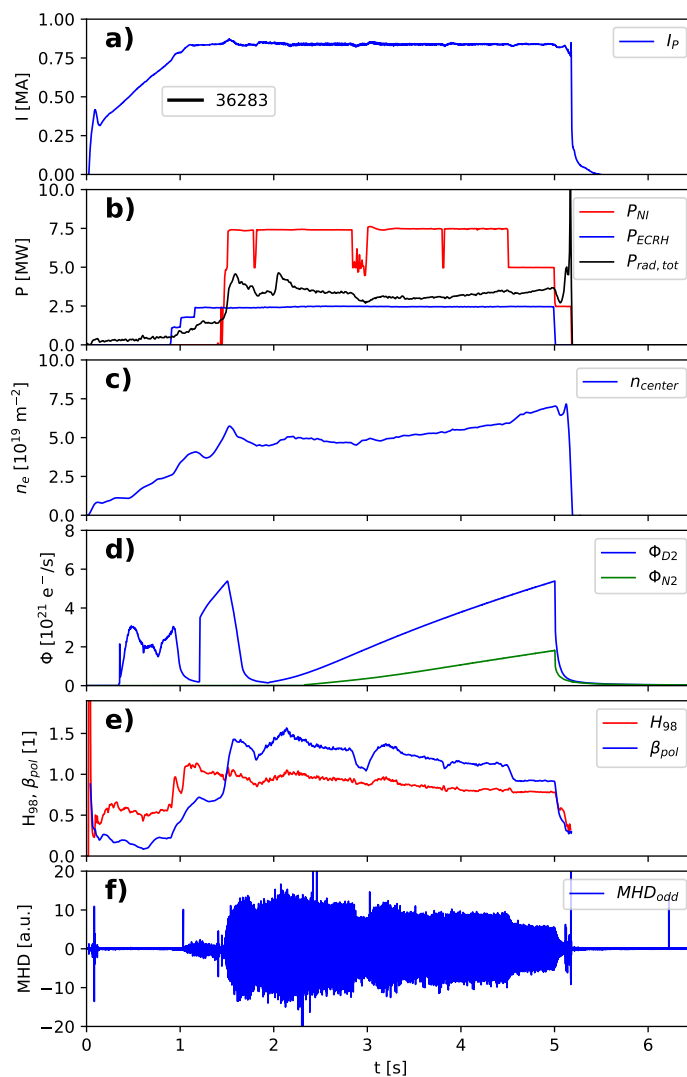


Figure 1: Several time traces of the USN H-mode discharge 36283 in ASDEX Upgrade.

current (a) and a toroidal field strength of  $B_t = +2.5$  T (i.e. in favorable drift direction). It was heated with  $P_{NBI} = 7.5$  MW neutral beam injection and  $P_{ECRH} = 2.5$  MW electron cyclotron resonance heating. The total radiation measured by the diode bolometers is of the order of 4 MW (Fig. 1 b), while the foil bolometers (not shown here) measure about 40% more. Due to the gas puff ramp of deuterium and nitrogen (Fig. 1 d) the density (Fig. 1 c) measured by interferometry is increasing over time. However, due to the fact that the current cryo pump is located far away from the upper divertor strike lines and likely also because there is rather strong MHD mode activity (Fig. 1 f) the density is difficult to control. Despite this mode activity, the confinement is not too bad ( $H_{98} = 1 \dots 0.8$ , Fig. 1 e). In any case a clear power detachment is observed at the inner target in an early phase of the discharge as well as at the outer one in a later phase with peak heat flux values of the order of  $1 \text{ MW/m}^2$  measured by IR thermography.

The magnetic equilibrium of this discharge at 3.5 s is reconstructed by the CLISTE equilibrium code [17] (cf. Fig. 2 left) according to the currents measured in the PF coils as well as the magnetic measurements. Assuming the same  $p'(\Psi)$  and  $ff'(\Psi)$  profiles, where  $p$  is the plasma pressure,  $f = B_\phi \cdot R$  the product of the toroidal magnetic field and the major radius,  $\Psi$  the poloidal flux and  $' = d/d\Psi$ , as in this upper SN case the alternative configurations in Fig. 2 right) were computed by a modified version of EQUIL (a predecessor of CLISTE [18]) with the PF coil currents indicated in the figure. These configurations are similar to those in Ref. [14] (where further details are discussed) except that 1) the current imbalance between Do1 and Do2 has been minimized modifying in particular the V3 coils (located at  $R = 3.6$  m,  $z = \pm 0.7$  m, i.e. outside the displayed range of the figure) in order to reduce the forces acting on them 2) the position of the X-point has been lowered by a few cm to increase the outer divertor leg length, 3) the outer clearance has been increased to reduce the power deposition onto the limiter and 4) a realistic current density distribution  $j_\phi = Rp' + \mu_0 ff'/R$  including currents in the SOL has been taken into account. Note that the ‘welding torch’ configuration shown in Fig. 1 of Ref. [14] is still possible but not shown here for the sake of brevity.

In summary the upgrade is expected to allow a detailed study of various alternative divertor configurations and a direct comparison to the lower conventional one in a high power machine under detached and pumped target conditions.

### Acknowledgement

This work has been carried out within the framework of the EUROfusion Consortium and has received funding from the Euratom research and training programme 2014-2018 and 2019-2020 under grant agreement No 633053. The views and opinions expressed herein do not necessarily reflect those of the European Commission.

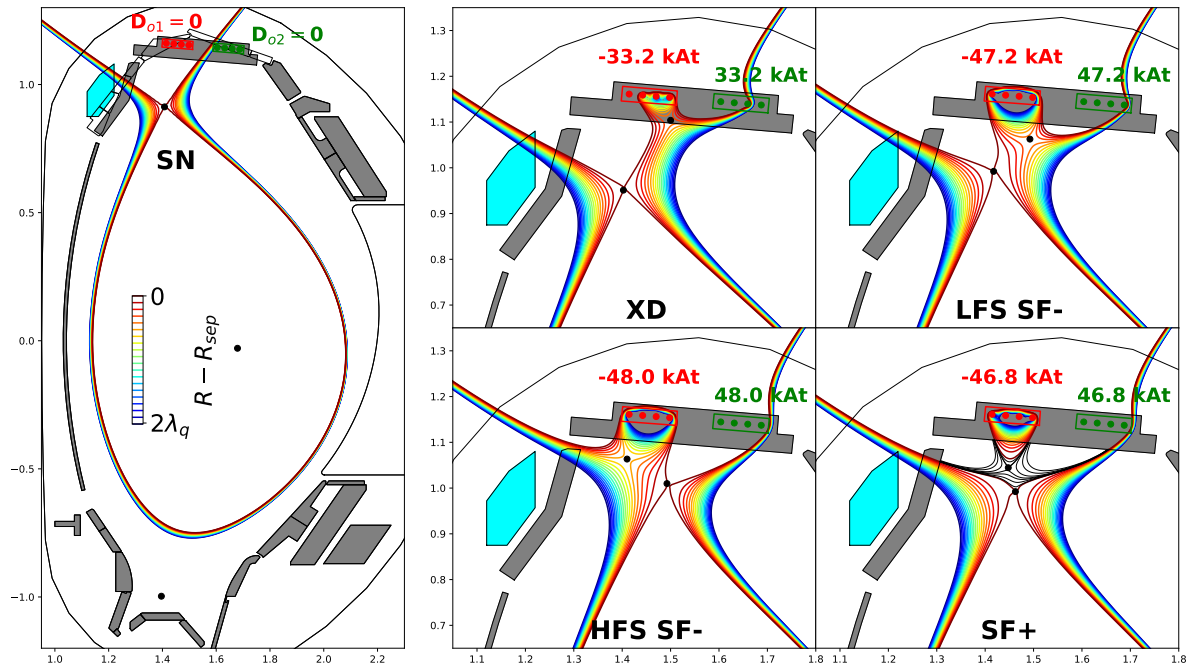


Figure 2: Upper divertor configurations possible after the planned modification of the upper divertor targets (old white, new grey) and the installation of the upper cryo-pump (cyan) in-vessel coils  $D_{o1}$  (red) and  $D_{o2}$  (green).

## References

- [1] Coda S. *et al.* 2017 *Nucl. Fus.* **57** 102011
- [2] Meyer H. *et al.* 2017 *Nucl. Fus.* **57** 102014
- [3] Wenninger R. *et al.* 2014 *Nucl. Fus.* **54** 114003
- [4] Soukhanovskii V.A. 1995 *Plasma Phys. Control. Fusion* **59** 064005
- [5] Ryutov D.D. 2007 *Phys. of Plasmas* **14** 064502
- [6] Lunt T. *et al.* 2014 *Plasma Phys. Control. Fusion* **56** 035009
- [7] Ryutov D.D. *et al.* 2014 *Phys. Scr.* **89** 088002
- [8] Lunt T. *et al.* 2016 *Plasma Phys. Control. Fusion* **58** 045027
- [9] Reimerdes H. *et al.* 2013 *Plasma Phys. Contr. Fusion* **55** 124027
- [10] Labit B. *et al.* 2017 *Nucl. Mat. and Energy* **12** 1015–1019
- [11] Pan O. *et al.* 2018 *Plasma Phys. Control. Fusion* **60** 085005
- [12] Reimerdes H. *et al.* 2017 *Nucl. Fus.* **57** 126007
- [13] Theiler Ch. *et al.* 2017 *Nucl. Fus.* **57** 072008
- [14] Lunt T. *et al.* 2017 *Nucl. Mat. and Energy* **12** 1037–1042
- [15] Herrmann A. *et al.* 2019 *Fus. Eng. Des.* *in press* doi:10.1016/j.fusengdes.2019.01.114
- [16] Lunt T. *et al.* 2019 *Nucl. Mat. and Energy* **19** 107–112
- [17] Mc Carthy P.J. 1999 *Phys. of Plasmas* **6** 3554
- [18] Lackner K. 1976 *Comp. Phys. Comm.* **12** 33–44